

## Pyrolysis Study of Cinnamaldehyde Model Compound with Analytical Py-GC×GC-FID/TOF-MS

Liang Li, Ruben Van de Vijver, Gorugantu SriBala, Junjie Weng, Kevin M. Van Geem\*

Laboratory for Chemical Technology, Department of Materials, Textiles and Chemical Engineering, Ghent University, Technologiepark 125, 9052 Gent, Belgium  
Kevin.VanGeem@ugent.be

Aldehyde-type lignin monomers like hydroxycinnamaldehydes are important monomers in plants downregulating the enzyme activity of cinnamyl alcohol dehydrogenase or catechol-O-methyltransferase. Cinnamaldehyde (CA) is the simplest aldehyde-type lignin model compound, which is also one of the primary products of cinnamic alcohol. In this contribution the experimental results obtained for the pyrolysis of *trans*-cinnamaldehyde (*trans*-CA) using a unique Py-GC×GC-FID/TOF-MS at temperatures from 573 to 1023 K are reported. Styrene and *cis*-cinnamaldehyde account for a large fraction of the total product yields at higher temperature. A dimer of styrene detected at higher temperatures ( $\geq 823$  K) suggests the presence of radical reactions. The plausible pyrolytic pathways of major products are proposed. This study is a first step towards a successive model extension to other aldehyde-type monomers such as *p*-coumaryl, coniferyl and sinapyl aldehydes.

### 1. Introduction

Lignocellulosic biomass fast pyrolysis is a promising thermochemical biomass conversion technology with high yields of bio-oil (up to 75 wt.%) (R.A. Sheldon, 2014; G. SriBala, H.H. Carstensen, et al., 2019). Bio-oil consists of several aromatic oxygenates which are of commercial importance. Recently, in-house studies demonstrated genetic engineering as a potential tool to alter the biomass composition for the increased production of value-added chemicals from lignin (G. SriBala, H.E. Toraman, et al., 2019; H.E. Toraman et al., 2018; H.E. Toraman et al., 2016). However, the lack of fundamental understanding of the lignin fast pyrolysis process makes it challenging to guide the genetic modification of biomass.

Lignin is a phenolic random polymer formed by dehydrogenative polymerization of monolignols: *p*-coumaryl alcohol, coniferyl alcohol, and sinapyl alcohol, which are phenolic derivatives of cinnamyl alcohol (A.J. Ragauskas et al., 2014). The monolignols are synthesized in plants by specific enzymatic pathways starting from phenylalanine (R. Van Acker et al., 2017). Due to the complexity and irregularity of the lignin structure, model compounds mimicking the essential reactive moieties in the lignin substrate are often selected and pyrolyzed (R.C. Brown et al., 2017; M. Pelucchi et al., 2018; S. Wang et al., 2017). Aldehyde-type lignin monomers such as hydroxycinnamaldehydes are incorporated into the lignin structure in a few genetically modified plants due to the downregulation of enzyme activity of cinnamyl alcohol dehydrogenase (*CAD*) or catechol-O-methyltransferase (*COMT*) (M. Özparpucu et al., 2018; R. Van Acker et al., 2017). Besides, cinnamaldehyde and coniferyl aldehyde were reported as the major products from the pyrolysis of cinnamyl alcohol and G-lignin (guaiacyl subunits), respectively (L. Khachatryan et al., 2016; T. Kotake et al., 2013). But there is a lack of *p*-coumaraldehyde in the pyrolysis products of *p*-coumaryl alcohol (R. Asatryan et al., 2017). Therefore, understanding the pyrolysis chemistry of these aldehydes can provide guidelines to plant genetic engineers that allow them to design and optimize lignocellulosic biomass for targeted chemicals by fast pyrolysis. The data can also contribute to the development of a detailed kinetic model for lignin thermal decomposition, especially to study the influence of primary products on the secondary pyrolysis. However, the pyrolysis of aldehyde-type lignin monomers has rarely been reported. Here, we studied the pyrolysis of *trans*-

cinnamaldehyde (*trans*-CA shown in Figure 1), the simplest aldehyde-type lignin model compound, which provides the main features of other aldehyde-type monomers: *p*-coumaryl, coniferyl and sinapyl aldehydes. The pyrolysis products from *trans*-CA was on-line investigated using a Py-GC×GC-FID/TOF-MS.

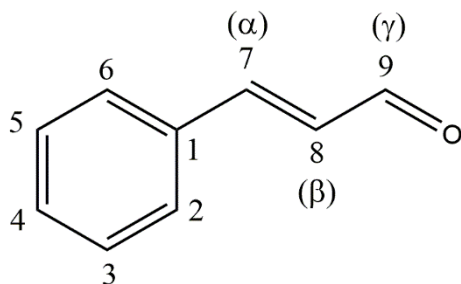


Figure 1: Chemical structure of *trans*-cinnamaldehyde.

## 2. Fast pyrolysis and on-line products analysis

*Trans*-CA (purity  $\geq 95\%$ , CAS: 104-55-2) was obtained from Sigma-aldrich, Inc. and used as is without further purification. The micro-pyrolysis setup is schematically represented in Figure 2 and comprises a reactor and an analytics section. The reactor consists of a double-shot tandem micro-pyrolyzer (Frontier Labs, Japan). In this study, only the first reactor was used to study the pyrolysis of *trans*-CA over a temperature range of 573–1023 K. The reactor has a deactivated quartz tube with an internal diameter of 4 mm up to a length of 75 mm and 2 mm for the rest of 45 mm. In a typical experiment, about 0.1 mg of *trans*-CA was loaded in a shallow eco-cup (4 mm length) and then the sample cups were inserted into the reactor via a dropping device. The samples in the cups were purged for 30 s with helium after which they were dropped into the preheated reactor manually at a set temperature and pyrolyzed for 5 min. A continuous flow of ultrahigh purity helium (the split flow of  $3.5 \times 10^{-6} \text{ m}^3/\text{s}$  with a split ratio of 100:1) was maintained to provide an inert atmosphere and sweep the pyrolysis products directly. The pyrolysis products from the reactor were collected and condensed for a specific period of time at the head of a deactivated guard column (ID:  $2.5 \times 10^4 \text{ m}$ ) with the help of a micro-jet cryogenic trap cooled with liquid nitrogen up to 77 K, as shown in Figure 2. Thereafter, the trap is heated under the set temperature programs and the products are split into two streams for the simultaneous analysis of permanent gases and water in a customized multicolumn GC (Trace 1300), and other products along with unreacted *trans*-CA in the GC × GC. The customized GC consists of a valve oven with a series of electrical depressurization valves (ELDVs) that are switched at pre-determined times, to regulate the injection of gases on to different GC columns.

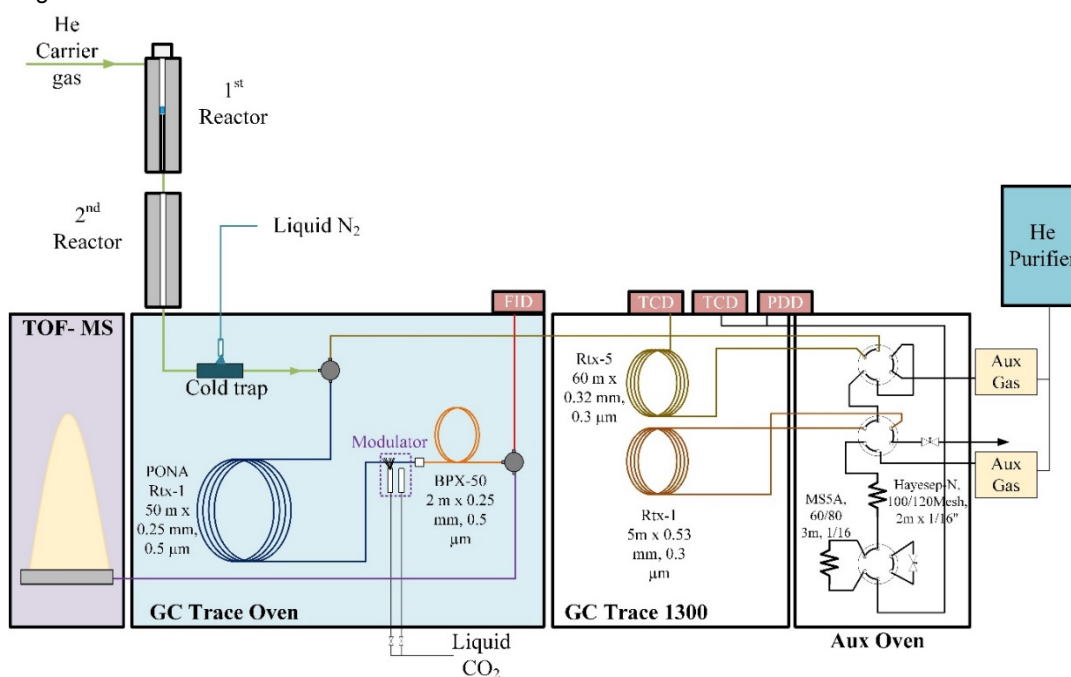


Figure 2: Schematic diagram of the micro-pyrolyzer reactor with a comprehensive analytical section.

The GC × GC (Thermo Scientific, Trace GC) consists of Rtx-1 PONA as the 1st column, and BPX-5 as the 2nd column and a two-stage modulator with liquid CO<sub>2</sub> jets to separate the products based on boiling points and polarity respectively. Details of the quantification of GC × GC data have been discussed elsewhere (M.R. Djokic et al., 2012; S.P. Pyl et al., 2011). The oven temperature was programmed from 313 K (6 min) to 573 K (2 min) at 278 K/min heating rate. A TOF-MS (BenchTOF-Select, Markes International) was used to identify the products with an ionization voltage of -20 eV. Finally, a flame ionization detector (FID, Thermo Scientific) was connected to quantify the product yields. The reactant *trans*-CA was calibrated externally and then all the other pyrolysis products were quantified according to the effective carbon number method (K. Schofield, 2008). Experiments under the same conditions were repeated at least three times.

### 3. Results and discussion

#### 3.1 Thermal degradation behavior of *trans*-CA

The decomposition profile of *trans*-CA shows (Figure 3a) that it hardly reacts at lower temperatures (< 773 K) and then rapidly decomposes above 773 K. There is still ~50% of the reactant in the final product distribution when the temperature reaches 1023 K. Compared with the pyrolysis profiles of cinnamyl alcohol that rapidly decomposes from 673 K (L. Khachatryan et al., 2016), the reactivity of *trans*-CA seems significantly lower. The role of the functional groups (-CH<sub>3</sub>OH and -CHO) in the pyrolysis process deserves further study.

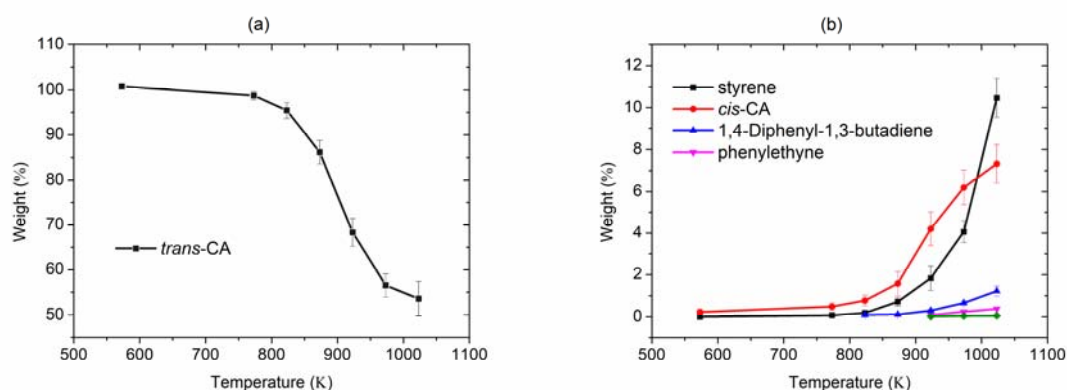


Figure 3: (a) Decomposition profiles of *trans*-CA. (b) Temperature-dependent product profiles evolved from *trans*-CA pyrolysis.

Table 1: Products formed from *trans*-CA pyrolysis at 1023 K.

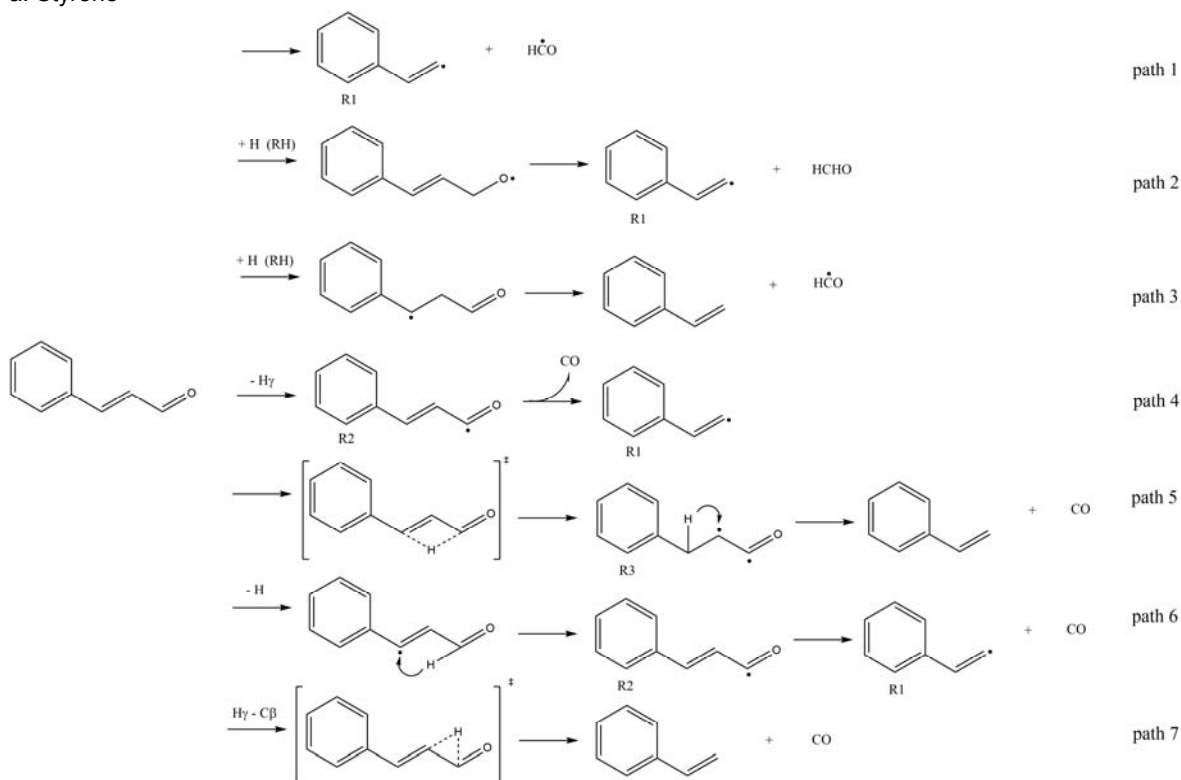
Compound no.	Retention time (min)	Name	Chemical formula	Yields (%)
1	7.33	acetaldehyde	C <sub>2</sub> H <sub>4</sub> O	0.091
2	10.33	benzene	C <sub>6</sub> H <sub>6</sub>	0.054
3	12.83	toluene	C <sub>7</sub> H <sub>8</sub>	0.013
4	15.58	ethylbenzene	C <sub>8</sub> H <sub>10</sub>	0.009
5	15.92	phenylethyne	C <sub>8</sub> H <sub>6</sub>	0.410
6	16.42	styrene	C <sub>8</sub> H <sub>8</sub>	11.507
7	20.67	benzene, 1-propenyl-	C <sub>9</sub> H <sub>10</sub>	0.014
8	20.75	benzeneacetaldehyde	C <sub>8</sub> H <sub>8</sub> O	0.020
9	21.25	benzene, 1-propynyl-	C <sub>9</sub> H <sub>8</sub>	0.015
10	26.08	<i>cis</i> -cinnamaldehyde	C <sub>9</sub> H <sub>8</sub> O	8.050
11	38.83	stilbene	C <sub>14</sub> H <sub>12</sub>	0.078
12	42.75	1,4-Diphenyl-1,3-butadiene	C <sub>16</sub> H <sub>14</sub>	1.339
13	27.67	<i>trans</i> -CA	C <sub>9</sub> H <sub>8</sub> O	53.583
14		water	H <sub>2</sub> O	3.344

About 15 pyrolysis products and unreacted *trans*-CA were experimentally identified and quantified at 1023 K (listed in Table 1). Water, carbon monoxide and carbon dioxide were identified by the customized GC. Where the quantification of CO and CO<sub>2</sub> needs further experiments. Only a few products such as styrene and *cis*-cinnamaldehyde account for a large fraction of the total product yields at this temperature. The temperature-dependent profiles of these major pyrolysis products are shown in Figure 3b. At about 993 K, equal amounts

of styrene and *cis*-CA were observed which suggests that the reactions forming above two products are competing pathways at high temperatures. A dimer of styrene, 1,4-diphenyl-1,3-butadiene, was detected at higher temperatures ( $\geq 823$  K), whose yield increased with increasing temperature. This dimer most likely is formed from the free radical reactions involving styrene radicals. This indicates the presence of radical chemistry at higher temperatures.

### 3.2 Reaction pathways for the major products.

#### a. Styrene



#### b. *Cis*-cinnamaldehyde

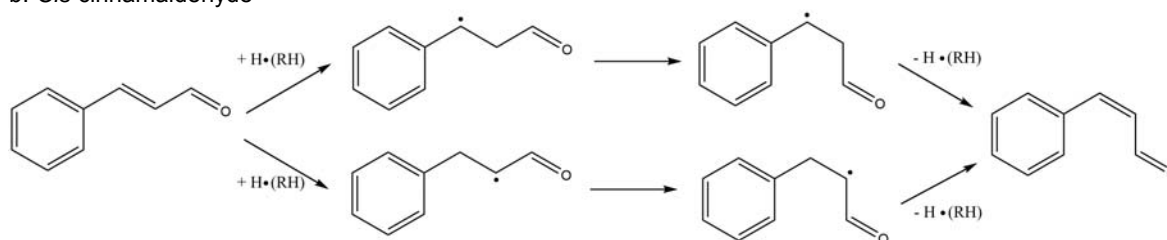
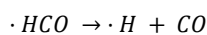


Figure 4: Proposed pyrolytic formation mechanisms of styrene and *cis*-CA from *trans*-CA.



Styrene and *cis*-CA are the major products from *trans*-CA pyrolysis and hence the reactions leading to their formation will be of primary interest in subsequent analysis of the decomposition pathways. The proposed formation mechanisms of styrene are shown in Figure 4a. There are seven plausible formation pathways of styrene. In path 1, *trans*-CA is converted directly to R1 via the homolysis of  $C_{\beta}-C_{\gamma}$  bond. In path 2, an oxygen-centered radical is formed firstly by H radical addition to oxygen atom of the *trans*-CA and then this intermediate undergoes  $\beta$ -scission to eliminate formaldehyde and to form R1. This pathway cannot be dominant because almost no formaldehyde was detected. In path 3, an intermediate radical is formed by H-addition to the double bond of the *trans*-CA then it converts to styrene via  $\beta$ -scission. In path 4, *trans*-CA firstly goes through dehydrogenation and converts to R2 via homolysis of  $C_{\gamma}-H$  bond. R2 then converts to R1 via a transition state. In path 5,  $H_{\gamma}$  shifts to  $C_{\alpha}$  via 4-centered transition state and R3 is formed. After that, styrene

and CO are formed via 1,2-H-shift and  $\beta$ -scission. In path 6, the H $\alpha$  of *trans*-CA is abstracted firstly, then H $\gamma$  transfers to C $\alpha$  to form R2. Subsequent reactions can refer to path 4. R1 formed during these pathways stabilizes either by H abstraction from a donor or recombines rapidly with a pool H radical to form the most abundant pyrolysis product styrene (> 10 % yields at 1023 K, Figure 3b). In addition to the free radical pathways, a concerted unimolecular pathway (path 7) for the formation of styrene is also proposed. In this pathway, *trans*-CA is directly converted to styrene and CO via 3-centered transition state. It should also be emphasized that almost all pathways except path 5 and 7 rely on the hydrogen radical or hydrogen donors in the vapors. Hence the reactions that can provide H radical or H-donors should be considered, such as the reaction (1) leading to the formation of H radical. The low energy barrier makes this reaction impossible to be ignored (K. Yasunaga et al., 2008).

The isomerization from *trans*-CA to *cis*-CA is possible via the radical mechanisms. As shown in Figure 4b, *trans*-CA firstly converts to C $\alpha$  or C $\beta$  radicals via the addition of hydrogen to the C $\beta$  or C $\alpha$  respectively. Subsequently, the radicals convert to *cis*-C $\alpha$  or *cis*-C $\beta$  radicals via the rotation of C $\alpha$ -C $\beta$  single bond. Then *cis*-C $\alpha$  or *cis*-C $\beta$  convert to *cis*-CA by a  $\beta$ -scission type elimination of the hydrogen radical from C $\beta$  or C $\alpha$ , respectively. This hydrogen radical could be used for addition to the double bond and make these pathways happen again.

Proposed pyrolytic formation mechanisms of 1,4-diphenyl-1,3-butadiene are presented in Figure 5. This dimer of styrene most likely comes from radical chemistry, such as the combination of two styrene radicals (path 1) or a free-radical propagation (path 2). According to quantitative analysis, this dimer is more likely to form at higher temperatures.

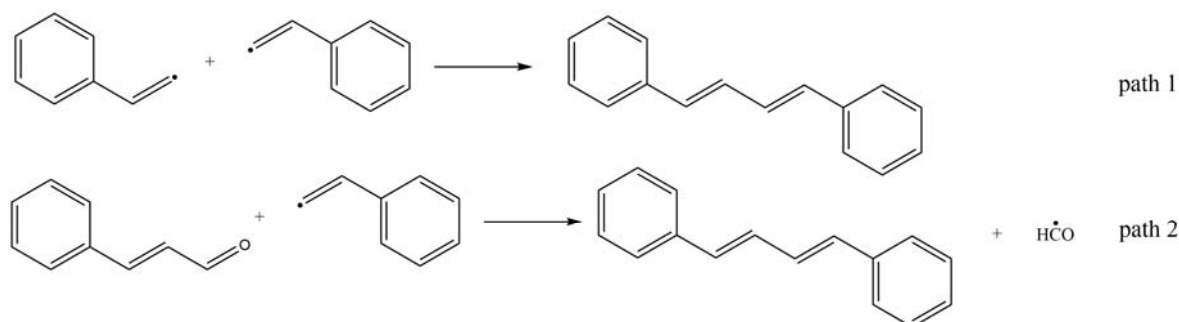


Figure 5: Proposed pyrolytic formation mechanisms of 1,4-diphenyl-1,3-butadiene.

#### 4. Conclusions

Analytical Py-GC $\times$ GC-FID/TOF-MS data demonstrated that the pyrolysis reactivity of *trans*-CA is low at temperatures below 773 K and it rapidly decomposes into styrene and *cis*-cinnamaldehyde for temperatures higher than 773 K. The plausible pyrolytic formation pathways of major products (styrene, *cis*-cinnamaldehyde) are proposed. Moreover, the formation of dimers of styrene, i.e., 1,4-diphenyl-1,3-butadiene, suggests the importance of radical chemistry at higher temperatures. A mechanistic study on *trans*-CA pyrolysis can shed light on the influence of the role on the secondary pyrolysis reactions occurring during the pyrolysis of lignin and form the basis towards a successive model extension to other aldehyde-type monomers such as *p*-coumaryl, coniferyl and sinapyl aldehydes. Furthermore, these models can provide guidelines to genetically modify biomass feedstocks for targeted chemicals by fast pyrolysis.

#### Acknowledgments

Liang Li thanks the financial support from the Overseas Study Program of Guangzhou Elite Project. The SBO proposal "Bioleum" supported by the Institute for Promotion of Innovation through Science and Technology in Flanders (IWT) is also acknowledged. Ruben Van de Vijver acknowledges financial support from the Fund for Scientific Research Flanders (FWO). The research leading to these results has received funding from the European Research Council under the European Union's Horizon 2020 research and innovation programme / ERC grant agreement n° 818607.

#### References

- Asatryan, R., Bennadji, H., Bozzelli, J.W., Ruckenstein, E., Khachatryan, L. 2017. Molecular products and fundamentally based reaction pathways in the gas-phase pyrolysis of the lignin model compound *p*-coumaryl alcohol. *The Journal of Physical Chemistry A*, 121(18), 3352-3371

- Brown, R.C., Wang, K. 2017. *Fast Pyrolysis of Biomass: Advances in Science and Technology* (Vol. 50): Royal Society of Chemistry.
- Djokic, M.R., Dijkmans, T., Yildiz, G., Prins, W., Van Geem, K.M. 2012. Quantitative analysis of crude and stabilized bio-oils by comprehensive two-dimensional gas-chromatography. *Journal of Chromatography A*, 1257, 131-140
- Khachatryan, L., Xu, M.-x., Wu, A.-j., Pechagin, M., Asatryan, R. 2016. Radicals and molecular products from the gas-phase pyrolysis of lignin model compounds. Cinnamyl alcohol. *Journal of Analytical and Applied Pyrolysis*, 121, 75-83
- Kotake, T., Kawamoto, H., Saka, S. 2013. Pyrolysis reactions of coniferyl alcohol as a model of the primary structure formed during lignin pyrolysis. *Journal of Analytical and Applied Pyrolysis*, 104, 573-584
- Özparpucu, M., Gierlinger, N., Burgert, I., Van Acker, R., Vanholme, R., Boerjan, W., Pilate, G., Déjardin, A., Rüggeberg, M. 2018. The effect of altered lignin composition on mechanical properties of cinnamyl alcohol dehydrogenase (CAD) deficient poplars. *Planta*, 247(4), 887-897
- Pelucchi, M., Faravelli, T., Frassoldati, A., Ranzi, E., Sribala, G., Marin, G.B., Van Geem, K.M. 2018. Experimental and kinetic modeling study of pyrolysis and combustion of anisole. *Chemical Engineering Transactions*, 65, 127-132
- Pyl, S.P., Schietekat, C.M., Van Geem, K.M., Reyniers, M.-F., Verammen, J., Beens, J., Marin, G.B. 2011. Rapeseed oil methyl ester pyrolysis: On-line product analysis using comprehensive two-dimensional gas chromatography. *Journal of Chromatography A*, 1218(21), 3217-3223
- Ragauskas, A.J., Beckham, G.T., Biddy, M.J., Chandra, R., Chen, F., Davis, M.F., Davison, B.H., Dixon, R.A., Gilna, P., Keller, M. 2014. Lignin valorization: improving lignin processing in the biorefinery. *science*, 344(6185), 1246843
- Schofield, K. 2008. The enigmatic mechanism of the flame ionization detector: Its overlooked implications for fossil fuel combustion modeling. *Progress in Energy and Combustion Science*, 34(3), 330-350
- Sheldon, R.A. 2014. Green and sustainable manufacture of chemicals from biomass: state of the art. *Green Chemistry*, 16(3), 950-963
- SriBala, G., Carstensen, H.H., Van Geem, K.M., Marin, G.B. 2019. Measuring biomass fast pyrolysis kinetics: State of the art. *Wiley Interdisciplinary Reviews: Energy and Environment*, 8(2), e326
- SriBala, G., Toraman, H.E., Symoens, S., Déjardin, A., Pilate, G., Boerjan, W., Ronsse, F., Van Geem, K.M., Marin, G.B. 2019. Analytical Py-GC/MS of Genetically Modified Poplar for the Increased Production of Bioaromatics. *Computational and Structural Biotechnology Journal*, 17, 599-610
- Toraman, H.E., Abrahamsson, V., Vanholme, R., Van Acker, R., Ronsse, F., Pilate, G., Boerjan, W., Van Geem, K.M., Marin, G.B. 2018. Application of Py-GC/MS coupled with PARAFAC2 and PLS-DA to study fast pyrolysis of genetically engineered poplars. *Journal of Analytical and Applied Pyrolysis*, 129, 101-111
- Toraman, H.E., Vanholme, R., Borén, E., Vanwonterghem, Y., Djokic, M.R., Yildiz, G., Ronsse, F., Prins, W., Boerjan, W., Van Geem, K.M. 2016. Potential of genetically engineered hybrid poplar for pyrolytic production of bio-based phenolic compounds. *Bioresource technology*, 207, 229-236
- Van Acker, R., Déjardin, A., Desmet, S., Hoengenaert, L., Vanholme, R., Morreel, K., Laurans, F., Kim, H., Santoro, N., Foster, C. 2017. Different routes for conifer- and sinapaldehyde and higher saccharification upon deficiency in the dehydrogenase CAD1. *Plant physiology*, 175(3), 1018-1039
- Wang, S., Dai, G., Yang, H., Luo, Z. 2017. Lignocellulosic biomass pyrolysis mechanism: a state-of-the-art review. *Progress in Energy and Combustion Science*, 62, 33-86
- Yasunaga, K., Kubo, S., Hoshikawa, H., Kamesawa, T., Hidaka, Y. 2008. Shock-tube and modeling study of acetaldehyde pyrolysis and oxidation. *International Journal of Chemical Kinetics*, 40(2), 73-102